The Intracellular Domain of the β2 Subunit Modulates the Gating of Cardiac $Na_v1.5$ Channels

Thomas Zimmer and Klaus Benndorf
Institute of Physiology II, Friedrich Schiller University, Jena, Germany

ABSTRACT We have previously shown that the transmembrane segment plus either the extracellular or intracellular domain of the β1 subunit are required to modify cardiac $Na_v1.5$ channels. In this study, we coexpressed the intracellular domain of the β2 subunit in a $\beta1/\beta2$ chimera with $Na_v1.5$ channels in *Xenopus* oocytes and obtained an atypical recovery behavior of $Na_v1.5$ channels not reported before for other Na^+ channels: Recovery times of up to 20 ms at -120 mV produced a similar fast recovery as observed for $Na_v1.5/\beta1$ channels, but the current amplitude decreased again at longer recovery times and reached a steady-state level after 1–2 s with current amplitudes of only 43 $\pm$ 2% of the value at 20 ms. Current reduction was accompanied by slowed inactivation and by a shift of steady-state activation toward depolarized potentials by 9 mV. All effects were reversible and they were not seen when deleting the β2 intracellular domain. These results describe the first functional effects of a β2 subunit region on $Na_v1.5$ channels and suggest a novel closed state in cardiac Na^+ channels accessible at hyperpolarized potentials.

INTRODUCTION

The α-subunits of mammalian voltage-gated Na^+ channels constitute a family of 10 different members (1) that are responsible for the initiation and propagation of action potentials in electrically excitable cells (2). These subunits interact with one or two small accessory β-subunits, thereby forming heteromultimeric protein complexes in the plasma membrane. As demonstrated by heterologous expression experiments, the α-subunit determines the main electrophysiological and pharmacological properties of a given Na^+ channel (2). Functional analysis on the known β-subunits revealed their multifunctional nature: first, β1 and β3 subunits shift steady-state gating, accelerate Na^+ current decay kinetics and recovery from inactivation, and increase the current amplitude of several α-subunits (3–17). The β1-induced gating effects on α-subunits strongly depend on the degree of sialylation of the extracellular β1 domain (18). Second, β1 subunits are capable of interfering with the action of fatty acids (19), pharmaceuticals (20), or natural toxins (21) on α-subunits. Third, β-subunits contain extracellular immunoglobulin (Ig) domains that are structurally homologous to the V-set of the Ig superfamily (22). They can act as cell adhesion molecules (CAM) (23) and recruit via intracellular interactions cytoskeletal proteins, such as ankyrin, to points of cell-cell contact (24). Thus, β-subunits serve as important communication links between the extracellular and intracellular environment of neurons. The conclusions from these in vitro studies were strongly supported by recent data on $\beta1^{(-/-)}$ and $\beta2^{(-/-)}$ knock-out mice (25–27). These experiments demonstrated not only the significance of both β-subunits for regulation of neuronal Na^+ channel density and localization, but also the fundamental function of β1 for nodal architecture and neurite outgrowth, thus pointing to the in vivo action of accessory β-subunits as CAM in the central and peripheral nerve system.

In the mammalian heart, the Na^+ channel isoform $Na_v1.5$ dominates the I_{Na} in atrial and ventricular cardiomyocytes (1,28). Studies on the subunit composition of cardiac Na^+ channels suggested an in vivo association of $Na_v1.5$ with β1 and β2 subunits (29). Immunocytochemical studies further demonstrated a remarkable cardiac expression of both β-subunits by Western blotting (29,30), and suggested a preferential colocalization of $Na_v1.5$ channels with β2 instead of β1 subunits at intercalated disks of ventricular cardiomyocytes (31). However, electrophysiological measurements in mammalian cell lines or *Xenopus* oocytes showed that only the β1 but not the β2 subunit exerts modulatory effects on $Na_v1.5$ gating (15,29). Thus, the lack of any electrophysiological effect of β2 on $Na_v1.5$ channels conflicts with the immunocytochemical data. A possible explanation could be that, in contrast to the situation in native cardiomyocytes, $Na_v1.5$ does not associate with β2 upon heterologous expression, as concluded from a missing colocalization of respectively labeled subunit constructs (32).

We observed previously that the β1 transmembrane segment was required for a current increase and for an accelerated recovery from inactivation of $Na_v1.5$ channels (15). To exert β1-like effects on $Na_v1.5$, either the extracellular or the intracellular domain of the β1 subunit was necessary in addition to the short membrane spanning region. For example, deletion of the β1 intracellular domain ($\beta1\Delta$) resulted in a faster recovery from inactivation and produced larger whole-cell currents, indicating that this shortened β1 variant still efficiently interacts with $Na_v1.5$. In contrast, modulatory

Submitted October 4, 2006, and accepted for publication January 17, 2007.

Address reprint requests to Thomas Zimmer, PhD, Institute of Physiology II, Friedrich Schiller University Kollegiengasse 9, 07743 Jena, Germany. Tel.: 49-3641-934372; Fax: 49-3641-933202; E-mail: thomas.zimmer@mti.uni-jena.de.

0006-3495/07/06/3885/08 $2.00

doi: 10.1529/biophysj.106.098889

effects of the $\beta 2$ subunit on $Na_v1.5$ are unknown. To create a functional channel complex in which the $\beta 2$ intracellular domain is in close contact with $Na_v1.5$, we attached this $\beta 2$ sequence to $\beta 11\Delta$ resulting in $\beta 112$. We expected that possible functional effects of the $\beta 2$ intracellular domain may become visible when the spatial requirements for an $\alpha/\beta 2$ interaction are fulfilled. In this study, we used such a β-subunit construct and observed severe modulation of $Na_v1.5$ function during recovery from inactivation that has not been observed in voltage-gated Na^+ channels before.

MATERIALS AND METHODS

cDNAs of Na^+ channel subunits

Plasmids pSP64T-hH1, pNa200, and pSPNaβ coding for human $Na_v1.5$ (hH1, accession No. M77235), for $Na_v1.2$ (rat brain IIA Na^+ channel, accession No. X61149), and for the rat $\beta 1$ subunit (accession No. M91808) were kindly provided by Dr. A. L. George (Vanderbilt University), Dr. A. L. Goldin (University of California), and Dr. W. Stühmer (Max Planck Institute, Göttingen), respectively. The $\beta 2$ subunit (accession No. U37026) was isolated by RT-PCR from the human brain astrocytoma cell line 1321N1, as previously described (32). The isolation of sequences for mouse $Na_v1.4$ (mH2; accession No. AJ278787) and mouse $Na_v1.5$ (mH1; accession No. AJ271477) has been previously described (33).

Recombinant DNA procedures

We subcloned the cDNAs of the $\beta 1$ and $\beta 2$ subunit, and of deletion variant $\beta 11\Delta$ into the in vitro transcription vector pGEMHEnew, resulting in plasmids pGEM-$\beta 1$, pGEM-$\beta 2$, and pGEM-$\beta 11\Delta$, as previously described (15). This vector contains the T7 promoter, a 5′-untranslated region (UTR) of the *Xenopus* β-globin gene and a multicloning site. To create the construct $\beta 112$, the desired $\beta 1$ and $\beta 2$ subunit regions were first separately amplified by PCR and then linked by a recombinant PCR step using the internal primer pair 5′-ACTTGACCACCATCTCCGCCACGAGCCATA-3′ and 5′-GGCGGAGATGGTGGTCAAGTGTGTGAGGAG-3′. The recombinant fragment was subcloned into the *Bam*HI/*Hin*dIII sites of pGEMHEnew resulting in pGEM-$\beta 112$. PfuTurbo DNA polymerase (Stratagene, La Jolla, CA) was used for all PCR reactions to minimize PCR-mediated nucleotide exchanges. The plasmid was expected to encode chimera $\beta 112$ consisting of amino acids M1–M178 of $\beta 1$ plus amino acids V179–K215 of $\beta 2$ (amino acid numbering according to the premature full-length proteins). Mouse $Na_v1.4$ was subcloned into pSP64T by releasing the hH1 coding region in pSP64T-hH1 using *Bgl*II/*Sma*I digestion and inserting a *Bam*HI/*Xho*I fragment of mouse $Na_v1.4$ (mH2) released from the respective pTSV40Gnew vector (33), resulting in plasmid pSP64T-m$Na_v1.4$. To allow for a respective blunt-end ligation, the *Xho*I site was treated with Klenow enzyme. Mouse $Na_v1.5$ was subcloned into a pSP64-PolyA derivative (Promega, Mannheim, Germany) by releasing the $\beta 1$ subunit region in pSPNaβ using *Hin*dIII/*Hin*cII digestion and inserting a *Hin*dIII/*Not*I fragment of mouse $Na_v1.5$ (mH1) released from pTSV40Gnew-mH1 (33) after treatment of the *Not*I site with Klenow enzyme, resulting in vector pSP-m$Na_v1.5$. The correctness of the DNA constructs was checked by the dideoxy DNA sequencing method.

Heterologous expression in *Xenopus* oocytes

Capped cRNAs were prepared by digestion of respective plasmids with *Not*I (pNa200 and pSP64T-m$Na_v1.4$), *Eco*RI (pSP-m$Na_v1.5$), *Spe*I (pSP64T-hH1), *Xba*I (pGEM-$\beta 1$ and pGEM-$\beta 11\Delta$), and *Hin*dIII (pGEM-$\beta 112$ and pGEM-$\beta 2$), followed by in vitro transcription reaction with SP6 (pSP64 derivatives) and T7 (pNa200 and all pGEM derivatives) RNA polymerase (Roche Diagnostics GmbH, Mannheim, Germany). Thus, the cRNAs of all Na^+ channel isoforms and of the β-subunit variants were composed of the β-globin 5′-UTR and the respective α- or β-subunit sequence.

Oocytes from *Xenopus laevis* were obtained as previously described (32). Glass micropipettes were used to inject a volume of capped cRNA per oocyte of ~40–60 nl. The final cRNA concentrations used to inject oocytes were 0.02 μg/μl ($Na_v1.5$) and 0.01 μg/μl ($Na_v1.2$, $Na_v1.4$). The different cRNAs encoding the β-subunit variants were at a concentration of ~0.1 μg/μl so that the final molar ratio of α- to β-subunit was ~1:50 at the cRNA level. Injected oocytes were incubated for 3 days at 18°C in Barth medium. Under those conditions the amplitudes of I_{Na}, measured 3 days after injection at the test potential of -25 mV ($Na_v1.5$) and −10 mV ($Na_v1.2$, $Na_v1.4$), were between 0.5 and 5.0 μA. The recovery from inactivation was determined from Na^+ currents with an amplitude between 1 and 4 μA.

Electrophysiology

Whole-cell Na^+ currents were recorded with the two-microelectrode voltage clamp technique using a commercial amplifier (OC725C, Warner Instruments, Hamden, CT). The glass microelectrodes were filled with 3 M KCl. The microelectrode resistance was between 0.2 and 0.5 MΩ. The bath solution contained (in mM): 96 NaCl, 2 KCl, 1.8 $CaCl_2$, 10 Hepes/KOH, pH 7.2. The currents were elicited by test potentials from −80 to 40 mV (holding potential of −120 mV). The pulsing frequency was 0.1 Hz. We used only cells that produced a peak current amplitude <5 μA. Steady-state activation (m_∞) was evaluated by fitting the Boltzmann equation $m_\infty = \{1 + \exp[-(V - V_m)/s]\}^{-1}$ to the normalized conductance as function of voltage. V is the test potential, V_m the midactivation potential, and s the slope factor in mV. Recovery from inactivation was determined with a standard protocol (Fig. 1) at a frequency of 0.1 Hz. Recording and analysis of the data were performed on a PC with the ISO2 software (MFK, Niedernhausen, Germany). The sampling rate was generally 20 kHz.

RESULTS

To test for a possible effect of the intracellular domain of the $\beta 2$ subunit on $Na_v1.5$, we attached this domain to the transmembrane plus extracellular domain of $\beta 1$, resulting in chimera $\beta 112$. We coexpressed the chimera with $Na_v1.5$ channels in *Xenopus* oocytes and investigated whole-cell currents by the two-microelectrode voltage-clamp technique. Coexpression of chimera $\beta 112$ produced an $Na_v1.5$ recovery behavior that was not seen before in any other voltage-gated Na^+ channel (Fig. 1, *bottom*): Short recovery intervals up to ~20 ms allowed $Na_v1.5$ channels to recover efficiently from inactivation resulting in increased current amplitudes. This process occurred almost as fast as in the case of $Na_v1.5/\beta 1$ channels (Fig. 2 *A*, *right*) and should be therefore mediated by $\beta 1$ regions in chimera $\beta 112$. Longer recovery intervals, however, led to a paradoxical decrease of the current (Fig. 1, *bottom*). After ~1 s, a steady-state current level with an amplitude of 43 ± 2% of the value at 20 ms was reached (Fig. 2 *A*, *left*). We observed this atypical recovery in both mouse and human $Na_v1.5$ channels coexpressed with $\beta 112$, but neither in $Na_v1.2$ nor in $Na_v1.4$ channels: Coexpression of $\beta 112$ with the neuronal or skeletal muscle isoform produced typical $\beta 1$-like effects, as accelerated recovery from inactivation (Fig. 2, *B* and *C*), increased current densities, and faster inactivation (data not shown). In conclusion,

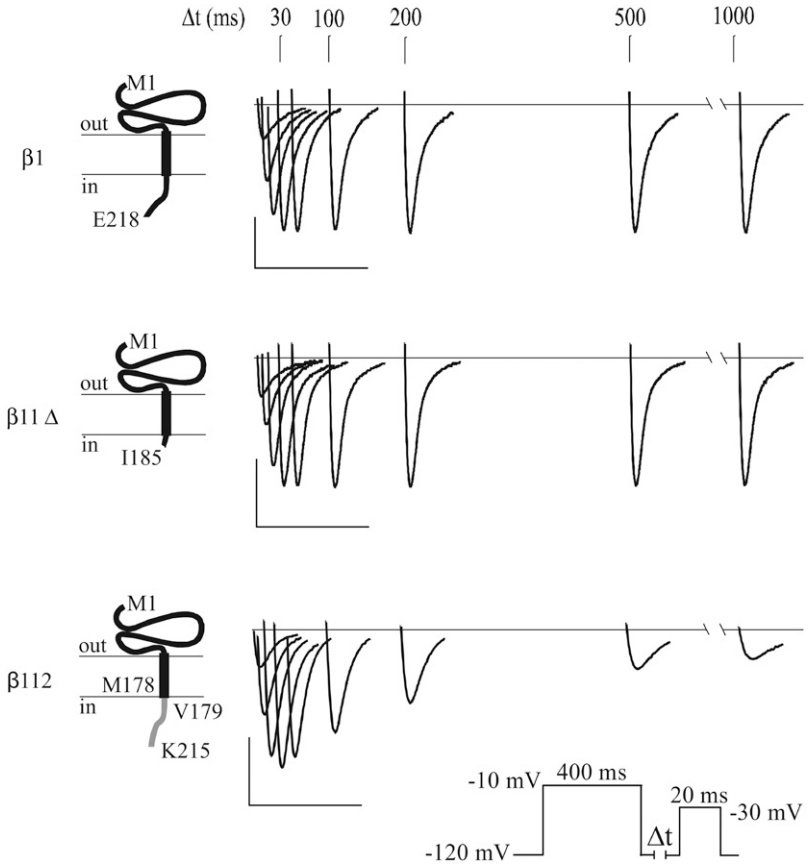

FIGURE 1 Atypical recovery from inactivation in $Na_v1.5$ channels produced by the intracellular domain of the $\beta2$ subunit in $\beta112$. The figure illustrates the domain structures of $\beta1$, $\beta11\Delta$, and $\beta112$, and the corresponding $Na_v1.5$ current traces at the indicated recovery intervals. The respective terminal amino acids of the $\beta1$ (*black*) and $\beta2$ (*gray*) subunit regions are indicated. We observed an accelerated recovery process and a current increase when coexpressing wild-type $\beta1$ subunit or deletion variant $\beta11\Delta$. Recovery time constants τ_{rec} determined with monoexponential fits were (in ms): 5.87 ± 0.18 for $Na_v1.5$, 3.20 ± 0.13 for $Na_v1.5/\beta1$, and 3.95 ± 0.29 for $Na_v1.5/\beta11\Delta$ (n = 8–15). Peak-current amplitudes relative to $Na_v1.5$ increased significantly by factor 3.47 ± 0.32 ($\beta1$) and 1.33 ± 0.15 ($\beta11\Delta$). Attachment of the $\beta2$ intracellular domain to the $\beta1$ transmembrane segment produced a paradoxical recovery behavior of wild-type $Na_v1.5$ channels. The pulse protocol is illustrated (pulse frequency 0.1 Hz). Calibration bars: 20 ms and 0.5 μA.

a close contact of cardiac-specific $Na_v1.5$ with the $\beta2$ intracellular domain led to a distinct interaction of both proteins, producing an atypical recovery from inactivation.

To exclude that an irreversible ''run-down'' caused the time-dependent current decrease at hyperpolarized potentials, we successively prolonged the recovery intervals Δt from 1 ms to 7 s, and shortened the time periods again from 7 s to 1 ms using the same oocyte. We found that the atypical recovery was reversible (Fig. 3).

We next investigated whether $Na_v1.5$ inactivation kinetics were affected by $\beta112$ (Fig. 4). After a recovery interval of 15 ms, inactivation time constants τ_h were similar for $Na_v1.5$, $Na_v1.5/\beta1$, and $Na_v1.5/\beta112$ channels (e.g., τ_h in ms at −25 mV: 2.05 ± 0.14 for $Na_v1.5$, 2.04 ± 0.08 for $Na_v1.5/\beta1$, and 2.17 ± 0.17 for $Na_v1.5/\beta112$; n = 5). At the same time, current amplitudes were significantly larger when coexpressing either $\beta1$ or $\beta112$, compared to cells expressing $Na_v1.5$ alone (Fig. 5 *A*). This current increase is mediated by the extracellular domain and the transmembrane segment of $\beta1$, because it was also found when coexpressing $\beta11\Delta$ (15). Upon longer recovery intervals, the $\beta2$ intracellular domain successively decreased the current amplitude and concomitantly decelerated the inactivation kinetics (Figs. 4 and 5 *B*). Interestingly, a minor deceleration of inactivation upon longer recovery intervals occurred also in $Na_v1.5$ and $Na_v1.5/\beta1$ channels (Fig. 4).

These data suggested that, upon interaction with the $\beta2$ intracellular domain, $Na_v1.5$ channels enter an additional closed state at hyperpolarized potentials in a time-dependent manner. As shown in Fig. 6, $Na_v1.5/\beta112$ channels captured in this closed state (−120 mV for 10 s) could not escape when stepping the voltage of the prepulse up to −80 mV: The currents at the test pulse were constant at nearly 30% of the maximal current. Further prepulse depolarizations allowed for a transition to the open and/or inactivated state during this prepulse. During the recovery pulse of 15 ms at −120 mV, channels recovered from inactivation. This interval was too short for a full transition to the additional closed state. Consequently, channel activation at the test pulse was facilitated and currents increased. Such an atypical recovery behavior was not observed in $Na_v1.5/\beta1$ channels: The 15-ms recovery interval was too short for a complete recovery of channels that were inactivated during the prepulse. Consequently, the current at the test pulse decreased (Fig. 6).

Reduced whole-cell currents and slowed inactivation in $Na_v1.5/\beta112$ channels at longer recovery intervals suggested that the current decrease during the recovery from inactivation is at least to some extent the result of a shift of steady-state activation toward depolarized potentials. To test this hypothesis, we compared steady-state activation curves at the recovery intervals of 15 and 4000 ms. At 15 ms, we obtained similar midactivation potentials (V_m) for $Na_v1.5$, $Na_v1.5/\beta1$,

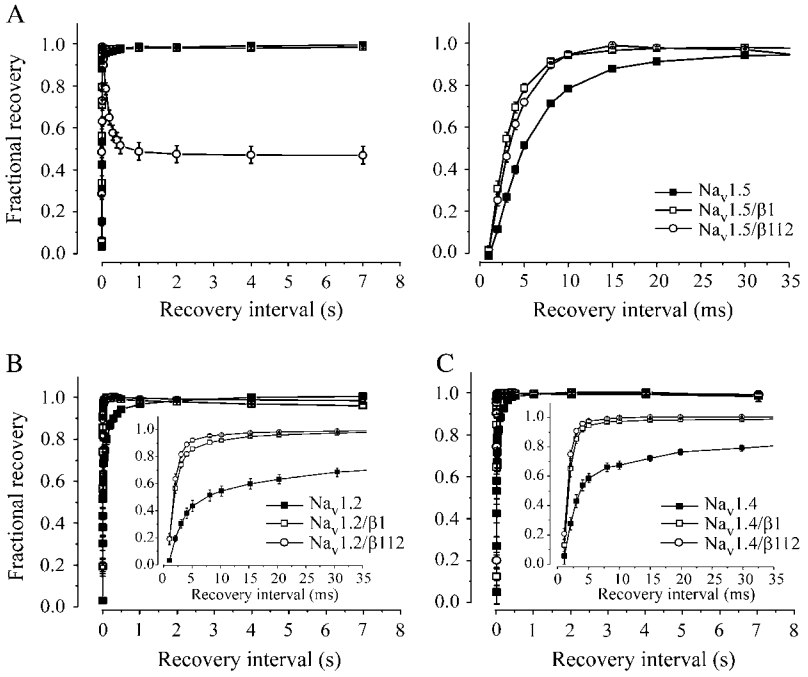

FIGURE 2 Recovery from inactivation in mouse $Na_v1.5$ (*A*), rat $Na_v1.2$ (*B*), and mouse $Na_v1.4$ (*C*) channels upon coexpression of $\beta112$. The figure shows that $Na_v1.5/\beta112$ currents decreased at recovery intervals >20 ms and reached a steady-state level after 1–2 s with current amplitudes of <50% of the value at 20 ms. In case of human $Na_v1.5$ very similar data were consistently obtained (data not shown). In $Na_v1.2$ and $Na_v1.4$ channels, an atypical recovery was not observed. Instead, the typical $\beta1$-like modulatory effect on recovery was obtained when coexpressing $\beta112$. Number of measurements: $n = 9$ for $Na_v1.5$, $n = 15$ for $Na_v1.5/\beta1$, $n = 15$ for $Na_v1.5/\beta112$, $n = 7$ for $Na_v1.2$, $n = 6$ for $Na_v1.2/\beta1$, $n = 6$ for $Na_v1.2/\beta112$, $n = 9$ for $Na_v1.4$, $n = 5$ for $Na_v1.4/\beta1$, and $n = 6$ for $Na_v1.4/\beta112$. For pulse protocol see Fig. 1 (test pulse to −30 mV for $Na_v1.5$, and to −20 mV for $Na_v1.2$ and $Na_v1.4$). Error bars represent mean ± SE.

and $Na_v1.5/\beta112$ channels (Table 1). At 4000 ms, V_m values did not change in case of $Na_v1.5$ and $Na_v1.5/\beta1$ channels ($p > 0.05$). In contrast, chimera $\beta112$ significantly shifted $Na_v1.5$ steady-state activation by ~9 mV to depolarized potentials (15 vs. 4000 ms; Table 1, Fig. 7). This shift can fully explain the observed whole-cell current reduction during recovery from inactivation. When applying a test pulse around the midactivation potential (−30 mV), the respective depolarized shift of the steady-state activation curve decreased the channel number responding to the voltage stimulus. Consequently, the phenomenon of reduced peak currents upon longer recovery intervals was not seen when applying a test pulse to 0 mV (Fig. 7 *C*). However, the altered steady-state activation alone cannot explain the significantly decelerated inactivation kinetics in $Na_v1.5/\beta112$ channels. Current decay time constant remained markedly larger also at test potentials more positive than 0 mV (Fig. 4).

Finally, we investigated the voltage dependence of the atypical recovery and compared the effect of two distant recovery potentials (−80 and −140 mV). As shown in Fig. 8 *A* (*left*), we observed a much faster initial recovery at −140 mV compared to −80 mV. In control experiments with $Na_v1.5/\beta1$ channels, recovery was much faster at the more hyperpolarized potential (Fig. 8 *A*, *right*) and both recovery potentials produced the maximal steady-state current level. In contrast to this, availability of $Na_v1.5/\beta112$ channels passed a maximum and reached finally a steady-state value at ~30% of the maximal current. Interestingly, this steady state was independent of the recovery potential: We observed a similar steady-state level at both −140 and −80 mV. Consequently, when investigating the effect of the $\beta2$ intracellular domain in $\beta112$ on both $Na_v1.5$ inactivation time course and steady-state activation, we obtained similar data for both potentials at long recovery intervals (Fig. 8, *B* and *C*). Therefore, we conclude that the channel transition to the additional closed state at potentials negative to −80 mV is voltage independent.

DISCUSSION

In this study we report the first functional effects of a specific $\beta2$ sequence on cardiac $Na_v1.5$ channels: The $\beta2$ intracellular domain is capable of generating an atypical recovery

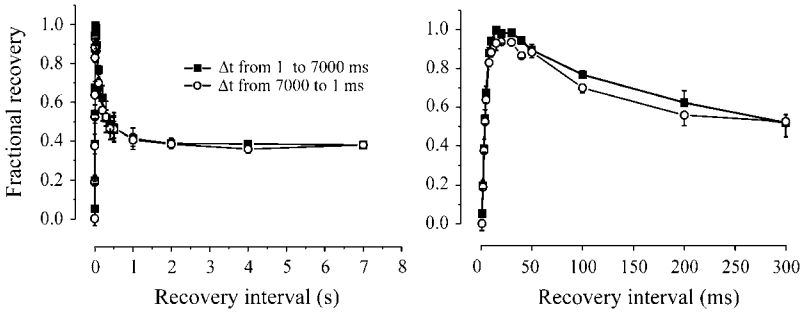

FIGURE 3 The atypical recovery in $Na_v1.5/\beta112$ channels was reversible. The recovery interval Δt was successively prolonged until 7 s (■) and then again shortened to 1 ms (○). The figure illustrates fractional recovery at intervals up to 7 s (*left*) and up to 300 ms (*right*). For pulse protocol see Fig. 1 ($n = 6$). Error bars represent mean ± SE.

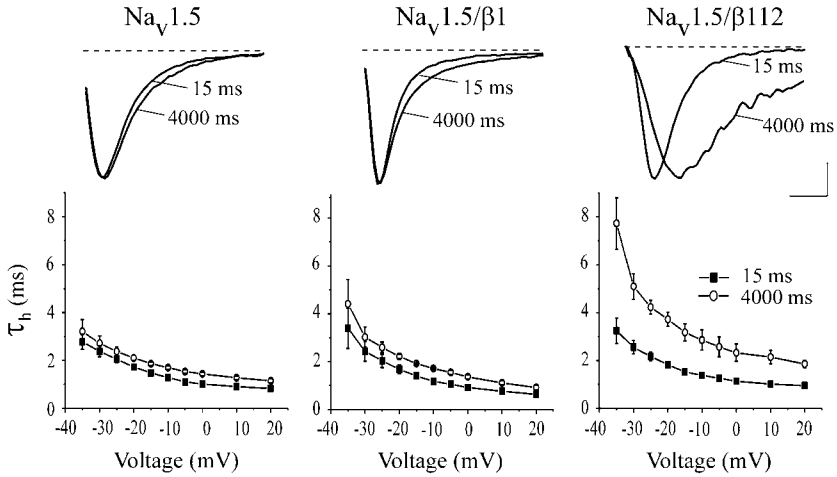

FIGURE 4 Effect of $\beta 112$ on inactivation kinetics of $Na_v1.5$ channels. Current traces from $Na_v1.5$, $Na_v1.5/\beta 1$, and $Na_v1.5/\beta 112$ channels at -25 mV, and corresponding plots of the inactivation time constants τ_h as function of voltage after recovery intervals of 15 ms (■) and 4000 ms (○). Please note that a significant deceleration of inactivation upon longer recovery intervals occurred also in $Na_v1.5$ and $Na_v1.5/\beta 1$ channels ($p < 0.05$ for τ_h values in ms at -10 mV: 1.29 ± 0.05 at 15 ms versus 1.70 ± 0.08 at 4000 ms for $Na_v1.5$, and 1.18 ± 0.07 at 15 ms versus 1.72 ± 0.04 at 4000 ms for $Na_v1.5/\beta 1$). Calibration bar is: 5 ms, and 0.9 μA for $Na_v1.5$, 1.9 μA for $Na_v1.5/\beta 1$, 1.0 μA for $Na_v1.5/\beta 112$ at 15 ms, and 0.3 μA for $Na_v1.5/\beta 112$ at 4000 ms. Number of experiments is: $n = 6$ for $Na_v1.5$, $n = 5$ for $Na_v1.5/\beta 1$, and $n = 5$ for $Na_v1.5/\beta 112$. Error bars represent mean ± SE.

behavior of cardiac $Na_v1.5$ channels. At longer recovery intervals the $\beta 2$ intracellular domain shifted steady-state activation toward depolarized potentials and decelerated channel inactivation (Figs. 4 and 7). Thus, the paradoxical current decrease upon longer recovery intervals observed at test potentials negative to -10 mV (e.g., -30 mV in Fig. 1) is not simply caused by an overshooting recovery from inactivation, as observed previously in voltage-gated K^+ channels (34). Our data suggest the existence of a novel closed state in $Na_v1.5$ channels accessible at hyperpolarized potentials that does neither occur in neuronal $Na_v1.2$ nor in skeletal muscle $Na_v1.4$ channels.

How can we interpret our results in terms of an $Na_v1.5$ gating model? We suggest that at hyperpolarized voltages, channels switch rapidly from the inactivated to the normal closed state in a voltage-dependent manner. This process is largely complete within 15–30 ms. After these short recovery intervals, channel activation produced current amplitudes and inactivation kinetics that were similar to those seen for $Na_v1.5/\beta 1$ channels (see increased current amplitudes upon coexpression of either $\beta 1$ or $\beta 112$ in Fig. 5 *A*). Prolongation of the recovery interval, however, favors a transition to an additional closed state, until a steady state is reached (after ~1 s). This transition is voltage independent at potentials negative to -80 mV (see Fig. 8). Channel activation from this additional closed state requires more positive voltages. At the same time, inactivation kinetics are decelerated. In conclusion, our data indicate that $Na_v1.5$ channels can be inactivated also by hyperpolarization. Inactivation kinetics have been demonstrated more than 20 years ago to be caused by the first latency of the channels (35). Single-channel analysis would be required to define the contribution of a possibly altered first latency to the biophysical phenomenon observed with $Na_v1.5/\beta 112$ channels. Significantly larger inactivation

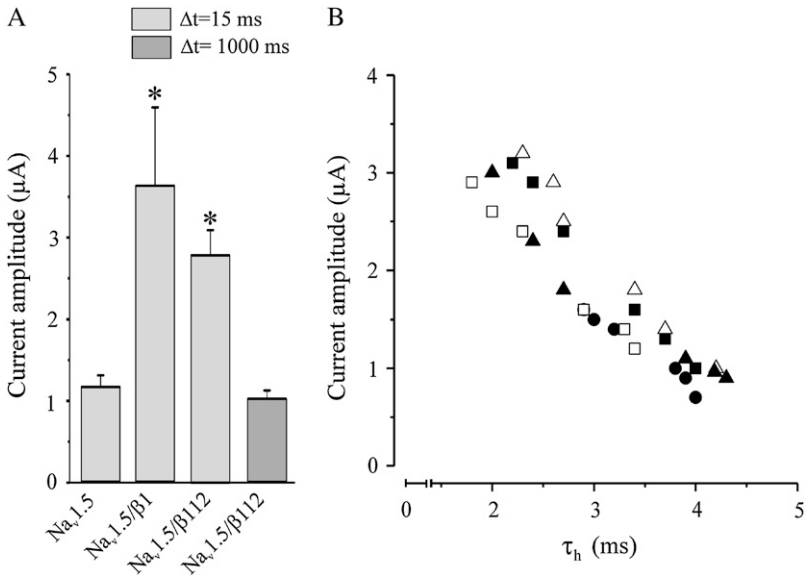

FIGURE 5 Effect of the $\beta 2$ intracellular domain on current amplitude and inactivation time constants in $Na_v1.5$ channels. (*A*) Current amplitudes at recovery intervals Δt of 15 and 1000 ms ($n = 5$ each). At $\Delta t = 15$ ms, the modulatory effect of the $\beta 1$ region on $Na_v1.5$ current amplitude can be observed also when coexpressing $\beta 112$ (* indicates $p < 0.05$ versus $Na_v1.5$ at 15 ms). However, at longer recovery intervals currents through $Na_v1.5/\beta 112$ channels decreased successively (compare also Fig. 1 to Fig. 3). (*B*) Current amplitude as a function of the inactivation time constant τ_h in $Na_v1.5/\beta 112$. The decreased current amplitudes upon longer recovery intervals are accompanied by decelerated inactivation. Data points were obtained from five independent measurements (illustrated by the *five different symbols*). The increase of τ_h was caused by successively prolonging the recovery interval (15, 50, 100, 300, 500, and 1000 ms; recovery potential, -120 mV).

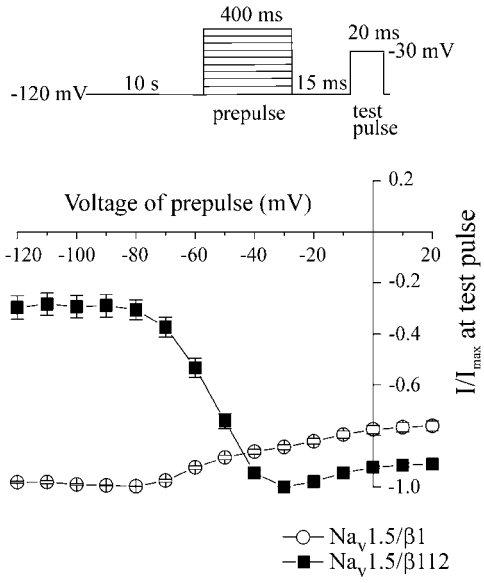

FIGURE 6 Effect of the prepulse potential on recovery of $Na_v1.5/\beta112$ channels at a short recovery interval (15 ms). The figure illustrates the relative current amplitude (normalized to −1) at the test pulse (−30 mV) as a function of the prepulse potential (from −120 to +20 mV). Number of measurements, $n = 7$ each. Error bars represent mean ± SE.

time constants at test pulse potentials positive to 0 mV suggest that also other single-channel properties are altered by $\beta112$: A test pulse to 0 mV increased whole-cell currents and decelerated inactivation kinetics upon longer recovery intervals (compare Figs. 4 and 7 *C*). It is interesting to note that a small $Na_v1.5$ channel fraction obviously enters the additional closed state also when coexpressing $\beta1$ or even in the absence of any other subunit (see decelerated inactivation at recovery interval of 4000 ms; *left* and *middle panel* in Fig. 4).

Although we measured currents through wild-type Na^+ channels, we used an artificial construct to provoke the unusual $Na_v1.5$ gating phenomenon. Consequently, our data raise the question why such an atypical recovery has not yet been observed when coexpressing wild-type $\beta2$? Previously, we found that $Na_v1.5$ and $\beta2$ are not colocalized upon heterologous expression (32), in contrast to immunocytochemical data obtained in cardiomyocytes (31). However, missing

TABLE 1 Midactivation potentials V_m after recovery intervals of 15 and 4000 ms

	V_m after recovery interval of		
Channel	15 ms (mV)	4000 ms (mV)	*n*
$Na_v1.5$	30.2 ± 1.2	29.5 ± 1.3	6
$Na_v1.5/\beta1$	27.4 ± 0.7	26.7 ± 0.7	5
$Na_v1.5/\beta112$	31.5 ± 1.0	22.5 ± 1.1*	8

A significant shift to depolarized potentials occurred only in $Na_v1.5/\beta112$ channels after a recovery interval of 4000 ms (*$p < 0.05$ for $Na_v1.5/\beta112$ channels at 15 vs. 4000 ms, and for $Na_v1.5$ versus $Na_v1.5/\beta112$ at 4000 ms). Data are presented as mean ± SE.

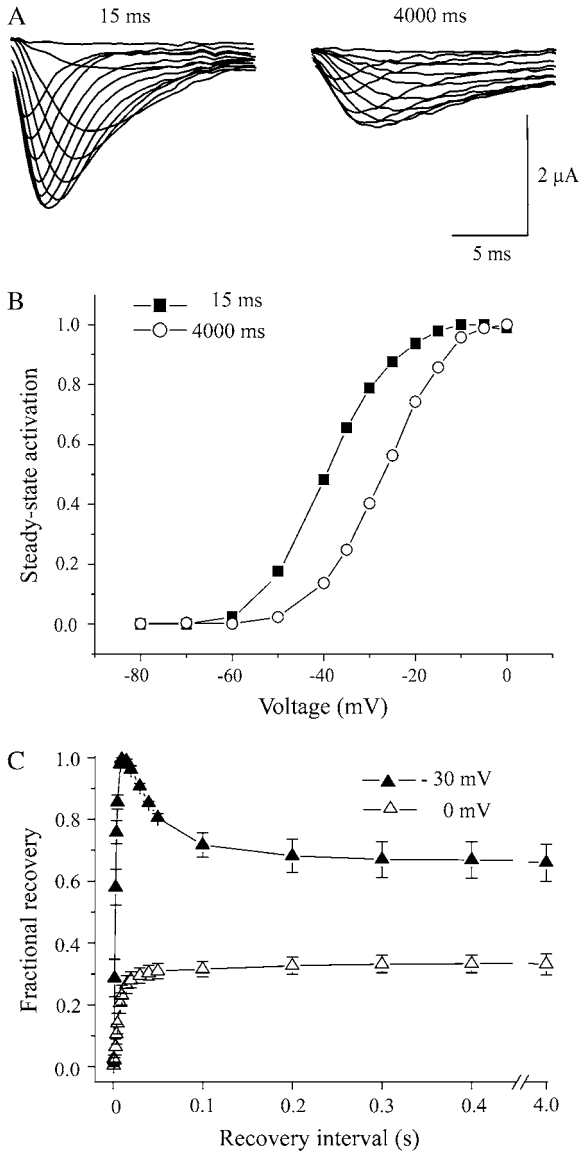

FIGURE 7 Longer recovery intervals shift steady-state activation in $Na_v1.5/\beta112$ channels. (*A*) Currents of $Na_v1.5/\beta112$ channels measured after the indicated recovery time points. (*B*) Representative steady-state activation curves in $Na_v1.5/\beta112$ channels for recovery intervals of 15 ms (■) and 4000 ms (○). For midactivation potentials (V_m) and statistics, see Table 1. (*C*) Recovery from inactivation in $Na_v1.5/\beta112$ channels at test potentials of 0 vs. −30 mV. Peak current reduction at −30 mV depended on the shift of the steady-state activation curve. At 0 mV, all available channels are activated and consequently, a current reduction was not obtained. Number of measurements, $n = 5$. All values were normalized with respect to the maximum current obtained at −30 mV.

colocalization is incompatible with an efficient intracellular assembly and trafficking of the channel complex to the plasma membrane, and thus also with a modulatory action of, respectively, associated β-subunits (15,32). When anchoring the intracellular domain of the $\beta2$ subunit to a $\beta1$ subunit deletion variant that interacts with $Na_v1.5$ ($\beta11\Delta$; (15)), we reconstituted a channel complex in which the $\beta2$ sequence

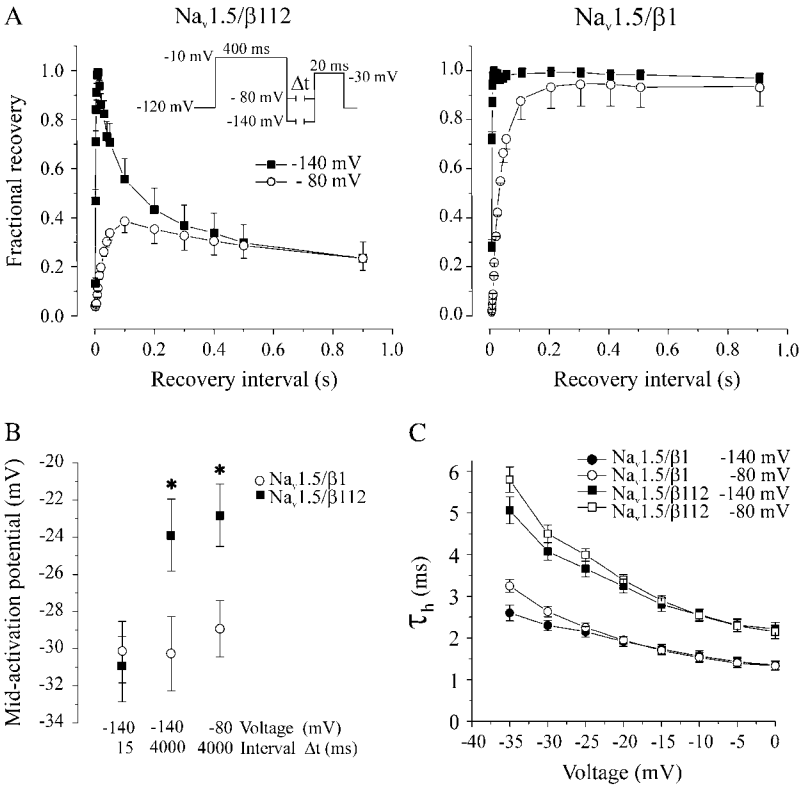

FIGURE 8 Atypical recovery from inactivation in $Na_v1.5/\beta112$ channels at recovery potentials of −140 and −80 mV. (*A*) Recovery from inactivation in $Na_v1.5/\beta112$ (*left*) and $Na_v1.5/\beta1$ (*right*) channels. Shorter intervals led to a faster recovery at the more hyperpolarized potential in both $Na_v1.5/\beta112$ and $Na_v1.5/\beta1$ channels. In contrast to $Na_v1.5/\beta1$, atypical recovery occurred in $Na_v1.5/\beta112$ at both −140 and −80 mV, resulting in similar current levels at intervals >0.3 s independently of the recovery potential. (*B*) Effect of the $\beta2$ intracellular domain on $Na_v1.5$ steady-state activation after long recovery intervals. A clear shift of steady-state activation occurred at −140 mV after longer recovery intervals (* $p < 0.05$; midactivation potentials V_m, −31.1 ± 1.8 mV at 15 ms versus −23.9 ± 1.9 mV at 4000 ms), similarly as observed at −120 mV (see Table 1). At 4000 ms, steady-state activation was similar at −80 mV (V_m, −22.8 ± 1.7 mV; $n = 16$) compared to −140 mV. Neither the recovery interval nor the recovery potential had an effect on $Na_v1.5/\beta1$ channels (at −140 mV, V_m = −30.2 ± 1.6 at 15 ms and −30.3 ± 2.0 at 4000 ms; at −80 mV, V_m = −28.9 ± 1.5 mV at 4000 ms; $n = 11$). (*C*) Inactivation time constant τ_h as function of voltage at a recovery interval of 4000 ms. Deceleration of inactivation occurred only in $Na_v1.5/\beta112$ and did not depend on the recovery potential ($n = 16$ for $Na_v1.5/\beta112$, $n = 11$ for $Na_v1.5/\beta1$). Error bars represent mean ± SE.

should interact with $Na_v1.5$. In respective control experiments, we investigated the subcellular localization of $Na_v1.5/\beta11\Delta$ and $Na_v1.5/\beta112$ channels using different variants of the green fluorescent protein, and we indeed observed a strict α/β colocalization that was not seen when using wild-type $\beta2$ (data not shown).

However, we have to consider that the $\beta2$ intracellular domain may not interact at the correct $\beta2$ binding site in $Na_v1.5$ when using chimera $\beta112$. It is imaginable that $\beta1$ and $\beta2$ normally bind distinct sites on α-subunits. Thus, it is possible that chimera $\beta112$ binds specifically at the $\beta1$ site, thereby directing the $\beta2$ intracellular domain to $Na_v1.5$ regions normally interacting with $\beta1$. Moreover, protein folding of the intracellular domain of $\beta2$ may be affected in the chimera, despite an obviously normal trafficking and correct localization in the plasma membrane of heterologous host cells. Consequently, the paradoxical recovery effect could be rather specific for the chimera and may not be produced in vivo by wild-type $\beta2$. The fact that the recovery behavior reported in this study has not been seen in native cardiac Na^+ channels before is consistent with this idea (36).

In conclusion, the results of our study provide more insight into the biophysical properties of wild-type $Na_v1.5$ channels by suggesting the existence of an additional closed state at hyperpolarized potentials that has not been detected so far. This state does neither exist in neuronal nor skeletal muscle Na^+ channels, providing further evidence for the unique feature of $Na_v1.5$ to interact with β-subunits also at intracellular regions. Further research is necessary to provide more insight into the nature of this additional closed state by identifying the interacting amino acid residues in $Na_v1.5$. At the same time we have to notice that conclusions on the physiological significance of our results for an in vivo $Na_v1.5/\beta2$ interaction in the heart are still strictly limited.

Note added in proof: Recently, Johnson and Bennett (37) reported a $\beta2$-mediated hyperpolarizing shift in $Na_v1.5$ gating that was dependent on the degree of protein sialylation. This novel effect of $\beta2$ on $Na_v1.5$ function is, however, mediated by the extracellular domains of the channel subunits and thus distinct from the recovery effect reported in the present study.

The authors thank Karin Schoknecht and Birgit Tietsch for excellent technical assistance.

This work was supported by the German Federal Ministry of Education and Research grant 01ZZ0105 IZKF Jena (project 4.12) to T.Z.

REFERENCES

1. Goldin, A. L. 2001. Resurgence of sodium channel research. *Annu. Rev. Physiol.* 63:871–894.
2. Catterall, W. A. 1992. Cellular and molecular biology of voltage-gated sodium channels. *Physiol. Rev.* 72:S15–S48.
3. Wallner, M., L. Weigl, P. Meera, and I. Lotan. 1993. Modulation of the skeletal muscle sodium channel α-subunit by the β_1-subunit. *FEBS Lett.* 336:535–539.
4. Makita, N., P. B. Bennett, and A. L. George. 1994. Voltage-gated Na^+ channel $\beta1$ subunit mRNA expressed in adult human skeletal muscle, heart, and brain is encoded by a single gene. *J. Biol. Chem.* 269:7571–7578.

5. Patton, D. E., L. L. Isom, W. A. Catterall, and A. L. Goldin. 1994. The adult rat brain β_1 subunit modifies activation and inactivation gating of multiple sodium channel α-subunits. *J. Biol. Chem.* 269:17649–17655.
6. Nuss, H. B., N. Chiamvimonvat, M. T. Perez-Garcia, G. F. Tomaselli, and E. Marban. 1995. Functional association of the β_1 subunit with human cardiac (hH1) and rat skeletal muscle (μ1) sodium channel α subunits expressed in *Xenopus* oocytes. *J. Gen. Physiol.* 106:1171–1191.
7. Qu, Y., L. L. Isom, R. E. Westenbroek, J. C. Rogers, T. N. Tanada, K. A. McCormick, T. Scheuer, and W. A. Catterall. 1995. Modulation of cardiac Na^+ channel expression in *Xenopus* oocytes by β1 subunits. *J. Biol. Chem.* 270:25696–25701.
8. Kupershmidt, S., T. Yang, and T. M. Roden. 1998. Modulation of cardiac Na^+ current phenotype by β1-subunit expression. *Circ. Res.* 83:441–447.
9. Smith, R. D., and A. L. Goldin. 1998. Functional analysis of the rat I sodium channel in *Xenopus* oocytes. *J. Neurosci.* 18:811–820.
10. Morgan, K., E. B. Stevens, B. Shah, P. J. Cox, A. K. Dixon, K. Lee, R. D. Pinnock, J. Hughes, P. J. Richardson, K. Mizuguchi, and A. P. Jackson. 2000. β3: An additional auxiliary subunit of the voltage-sensitive sodium channel that modulates channel gating with distinct kinetics. *Proc. Natl. Acad. Sci. USA.* 97:2308–2313.
11. Qu, Y., R. Curtis, D. Lawson, K. Gilbride, P. Ge, P. S. DiStefano, I. Silos-Santiago, W. A. Catterall, and T. Scheuer. 2001. Differential modulation of sodium channel gating and persistent sodium currents by the β1, β2, and β3 subunits. *Mol. Cell. Neurosci.* 18:570–580.
12. Shah, B. S., E. B. Stevens, R. D. Pinnock, A. K. Dixon, and K. Lee. 2001. Developmental expression of the novel voltage-gated sodium channel auxiliary subunit β3, in rat CNS. *J. Physiol.* 534:763–776.
13. Stevens, E. B., P. J. Cox, B. S. Shah, A. K. Dixon, P. J. Richardson, R. D. Pinnock, and K. Lee. 2001. Tissue distribution and functional expression of the human voltage-gated sodium channel β3 subunit. *Pflugers Arch.* 441:481–488.
14. Meadows, L. S., Y. H. Chen, A. J. Powell, J. J. Clare, and D. S. Ragsdale. 2002. Functional modulation of human brain $Na_v1.3$ sodium channels, expressed in mammalian cells, by auxiliary beta1, beta2 and beta3 subunits. *Neuroscience.* 1144:745–753.
15. Zimmer, T., and K. Benndorf. 2002. The human heart and rat brain IIA Na^+ channels interact with different molecular regions of the β1 Subunit. *J. Gen. Physiol.* 120:887–895.
16. Vijayaragavan, K., A. J. Powell, I. J. Kinghorn, and M. Chahine. 2004. Role of auxiliary beta1-beta2-, and beta3-subunits and their interaction with Nav1.8 voltage-gated sodium channel. *Biochem. Biophys. Res. Commun.* 319:531–540.
17. Ko, S.-H., P. W. Lenkowski, H. C. Lee, J. P. Mounsey, and M. K. Patel. 2005. Modulation of $Na_v1.5$ by β1- and β3-subunit co-expression in mammalian cells. *Pflugers Arch.* 449:403–412.
18. Johnson, D., M. L. Montpetit, P. J. Stocker, and E. S. Bennett. 2004. The sialic acid component of the β1 subunit modulates voltage-gated sodium channel function. *J. Biol. Chem.* 279:44303–44310.
19. Xiao, Y.-F., S. N. Wright, G. K. Wang, J. P. Morgan, and A. Leaf. 2000. Coexpression with β1-subunit modifies the kinetics and fatty acid block of hH1α Na^+ channels. *Am. J. Physiol. Heart Circ. Physiol.* 279:H35–H46.
20. Makielski, J. C., J. T. Limberis, S. Y. Chang, Z. Fan, and J. W. Kyle. 1996. Coexpression of beta 1 with cardiac sodium channel alpha subunits in oocytes decreases lidocaine block. *Mol. Pharmacol.* 49:30–39.
21. Messner, D. J., and W. A. Catterall. 1986. The sodium channel from rat brain. Role of the β1 and β2 subunits in saxitoxin binding. *J. Biol. Chem.* 261:211–215.
22. Isom, L. L., D. S. Ragsdale, K. S. De Jongh, R. E. Westenbroek, B. F. X. Reber, T. Scheuer, and W. A. Catterall. 1995. Structure and function of the β_2 subunit of brain sodium channels, a transmembrane glycoprotein with a CAM motif. *Cell.* 83:433–442.
23. Ratcliffe, C. F., R. E. Westenbroek, R. Curtis, and W. A. Catterall. 2001. Sodium channel β1 and β3 subunits associate with neurofascin through their extracellular immunoglobulin-like domain. *J. Cell Biol.* 154:427–434.
24. Malhotra, J. D., K. Kazen-Gillespie, M. Hortsch, and L. L. Isom. 2000. Sodium channel β subunits mediate homophilic cell adhesion and recruit ankyrin to points of cell-cell contact. *J. Biol. Chem.* 275:11383–11388.
25. Chen, C., V. Bharucha, Y. Chen, R. E. Westenbroek, A. Brown, J. D. Malhotra, D. Jones, C. Avery, P. J. Gillespie, K. A. Kazen-Gillespie, K. Kazarinova-Noyes, P. Shrager, et al. 2002. Reduced sodium channel density, altered voltage dependence of inactivation, and increased susceptibility to seizures in mice lacking sodium channel beta 2-subunits. *Proc. Natl. Acad. Sci. USA.* 99:17072–17077.
26. Chen, C., R. E. Westenbroek, X. Xu, C. A. Edwards, D. R. Sorenson, Y. Chen, D. P. McEwen, H. A. O'Malley, V. Bharucha, L. S. Meadows, G. A. Knudsen, A. Vilaythong, et al. 2004. Mice lacking sodium channel beta1 subunits display defects in neuronal excitability, sodium channel expression, and nodal architecture. *J. Neurosci.* 24:4030–4042.
27. Davis, T. H., C. Chen, and L. L. Isom. 2004. Sodium channel β1 subunits promote neurite outgrowth in cerebellar granule neurons. *J. Biol. Chem.* 279:51424–51432.
28. Balser, J. R. 2001. The cardiac sodium channel: gating function and molecular pharmacology. *J. Mol. Cell. Cardiol.* 33:599–613.
29. Malhotra, J. D., C. Chen, I. Rivolta, H. Abriel, R. Malhotra, L. N. Mattei, F. C. Brosius, R. S. Kass, and L. L. Isom. 2001. Characterization of sodium channel α- and β-subunits in rat and mouse cardiac myocytes. *Circulation.* 103:1303–1310.
30. Sutkowski, E. M., and W. A. Catterall. 1990. β1 subunits of sodium channels. Studies with subunit-specific antibodies. *J. Biol. Chem.* 265:12393–12399.
31. Maier, S. K. G., R. E. Westenbroek, K. A. McCormick, R. Curtis, T. Scheuer, and W. A. Catterall. 2004. Distinct subcellular localization of different sodium channel α and β subunits in single ventricular myocytes from mouse heart. *Circulation.* 109:1421–1427.
32. Zimmer, T., C. Biskup, C. Bollensdorff, and K. Benndorf. 2002. The β1 subunit but not the β2 subunit colocalizes with the human heart Na^+ channel (hH1) already within the endoplasmic reticulum. *J. Membr. Biol.* 186:13–21.
33. Zimmer, T., C. Bollensdorff, V. Haufe, E. Birch-Hirschfeld, and K. Benndorf. 2002. Mouse heart Na^+ channels: primary structure and function of two isoforms and alternatively spliced variants. *Am. J. Physiol. Heart Circ. Physiol.* 282:H1007–H1017.
34. Wettwer, E., G. J. Amos, H. Posival, and R. Ravens. 1994. Transient outward current in human ventricular myocytes of subepicardial and subendocardial origin. *Circ. Res.* 75:473–482.
35. Aldrich, R. W., D. P. Corey, and C. F. Stevens. 1983. A reinterpretation of mammalian sodium channel gating based on single channel recordings. *Nature.* 306:436–441.
36. Benndorf, K., and B. Nilius. 1987. Inactivation of sodium channels in isolated myocardial mouse cells. *Eur. Biophys. J.* 15:117–127.
37. Johnson, D., and E. S. Bennett. 2006. Isoform-specific effects of the β2 subunit on voltage-gated sodium channel gaiting. *J. Biol. Chem.* 281: 25875–25881.